CLEARINGHOUSE FOR FEDERAL SCIENTIFIC AND TECHNICAL INFORMATION CFSTI
DOCUMENT MANAGEMENT BRANCH 410.11

LIMITATIONS IN REPRODUCTION QUALITY

ACCESSION # AD 604 409

☒ 1. WE REGRET THAT LEGIBILITY OF THIS DOCUMENT IS IN PART UNSATISFACTORY. REPRODUCTION HAS BEEN MADE FROM BEST AVAILABLE COPY.

☒ 2. A PORTION OF THE ORIGINAL DOCUMENT CONTAINS FINE DETAIL WHICH MAY MAKE READING OF PHOTOCOPY DIFFICULT.

☐ 3. THE ORIGINAL DOCUMENT CONTAINS COLOR, BUT DISTRIBUTION COPIES ARE AVAILABLE IN BLACK-AND-WHITE REPRODUCTION ONLY.

☐ 4. THE INITIAL DISTRIBUTION COPIES CONTAIN COLOR WHICH WILL BE SHOWN IN BLACK-AND-WHITE WHEN IT IS NECESSARY TO REPRINT.

☐ 5. LIMITED SUPPLY ON HAND: WHEN EXHAUSTED, DOCUMENT WILL BE AVAILABLE IN MICROFICHE ONLY.

☐ 6. LIMITED SUPPLY ON HAND: WHEN EXHAUSTED DOCUMENT WILL NOT BE AVAILABLE.

☐ 7. DOCUMENT IS AVAILABLE IN MICROFICHE ONLY.

☐ 8. DOCUMENT AVAILABLE ON LOAN FROM CFSTI (TT DOCUMENTS ONLY).

☐ 9.

PROCESSOR: PM

TSL-107-10/64

Technical Report No. 9

to

The Office of Naval Research

Contract Nonr-2296(03)
Amendm. No. 4

337

Solubility of H in Zr at Room Temperature and Properties of the Solid Solutions

by

M.E. Straumanis and D.H. Wiebe

Department of Metallurgical Engineering
of the University of Missouri at Rolla
School of Mines and Metallurgy
Rolla, Missouri

August, 1964

Solubility of H in Zr at Room Temperature

and

Properties of the Solid Solutions

Abstract

The α-ZrH_x samples were prepared from reactor grade zirconium hydride by decomposing it in a hydrogen atmosphere at various temperatures between 750 and 1000°C and by slowly cooling them to room temperature in vacuum.

The solid solubility limit of H in α-Zr in such samples was 310 ppm at room temperature, determined by the parametric X-ray method. About the same solid solubility limits (280 ppm) could be derived from the increase of tensile and yeild strength of Zr-wires with increasing content of H; within the solid solubility range the strength of the wires increased only slightly but increased strongly in the 2 phase region.

The solubility limit mentioned may also represent the H-solubility at 375°C, as it is virtually impossible to remove the H from the Zr below that temperature. This feature explains the discrepancy with thermodynamic measurements, which give only 10 ppm of H solubility at room temperature. However,

lattice parameter plots showed that no other phase segregated from ZrH_x solid solutions up to concentration of 310 ppm H.

It was found that the a-constant of pure Zr increases from a_{25} = 3.2360 to 3.2378 Å for Zr containing 310 ppm H in solid solution, and the c_{25} constant - from 5.1508 up to 5.1572 Å respectively. Beyond 310 ppm H both constants did not change.

The thermal expansion coefficients of α-$ZrH_{0.011}$ (containing 122 ppm H) between 15 and 55°C are: $\gamma_a = 4.6 \times 10^{-6}$ and $\gamma_c = 11.0 \times 10^{-6}\ °C^{-1}$.

The density of pure Zr was found to be 6.481, while the X-ray density was 6.4840 g cm^{-3} at 25°C. The experimental density decreased with increasing H-content more strongly than the X-ray density. This result points toward the increase of vacancy aggregations (while the H is absorbed in the α-ZrH_x. If these aggregations are noted in terms of vacant sites, then their number increases from nearly zero (for pure Zr) up to 0.014 sites/unit cell for Zr saturated with H.

At a certain excess of H, the vacancy clusters may serve as nucleation centers for the hydride phase. As this phase occupies a larger space than the matrix, from which the former is formed, microcracks may appear in the solid solution, causing the hydrogen embrittlement of the latter. The pile-up of dislocation may have the same effect.

INTRODUCTION

The presence of H in Zr has a deleterious effect on the mechanical properties of the metal, particularly as related to impact, creep, and fatigue[1-3]. Therefore, solubility determinations have been carried out by a number of investigators. Early work[4] showed an abrupt change in H solubility at the allotropic transition of Zr at 862°C. Later a thorough investigation was made of the Zr-H system at pressures of 1-760 mm Hg from room temperature to 1050°C[5]. Extrapolation of the data to low pressures, along with other solubilities calculated from diffusion studies in the range of 400 - 500°C, were reported in a discussion of the properties of Zr-H in alloys[1]. Gulbransen and Andrew[6] studied rather extensively the equilibrium and terminal solubilities of H in α-Zr in the range 425 - 600°C at pressures of about 0,001 - 0,1 mm Hg. Edwards, Leveseque, and Cubicciotti[7] determined the solid solution equilibria in the Zr-H system and presented a partial phase diagram of the system. H-solubilities were determined at H pressures of 1-760 mm Hg in the range 600 - 900°C. A phase diagram based on the data obtained by Schwartz and Mallett[1], was published by Vaughan and Bridge[8]. Ells and McQuillan[9] measured the H equilibrium pressure for a series of Zr-H alloys and established the partial constitutional

diagram of the Zr-H system. This diagram shows that the solubility of hydrogen in α-Zr varies markedly with temperature. The maximum solubility of hydrogen in α-Zr was found to be about 6% in the range of 500 to 550°C. Mallett and Albrecht[1] determined low pressure H-solubilities (0,1 - 4 μ Hg) in α- and β-Zr and in Zr-o alloys at 700° - 1000°C. Libowitz[11] carried out a pressure-composition-temperature study at high H contents in the temperature range of 500 - 800°C. More recently Motz[12] made some thermoanalytic, dilatometric and high temperature X-ray studies with alloys containing more then 40 at o/o H, simultaneously measuring the H pressure.

The solubilities at room temperature were obtained from those at high temperatures by extrapolation. E.g. from the diagram Fig. 1, it was concluded that the terminal solubility of H at low pressures at room temperature in α-Zr is about 10 ppm. As can be seen, such an extrapolation is not very certain.

The purpose of the present study was, therefore, to find this maximum solubility limit of H in α-Zr at room temperature and to explore some physical properties of these solid solutions. The study involved the determination of:

1. The precise lattice parameters of α-Zr at room temperature, charged with different amounts of hydrogen,

2. The coefficients of thermal expansion of hydrogen containing α-Zr,

3. The densities of different Zr-H samples in the solid solution range,

4. The tensile properties of Zr (at room temperature) containing various amounts of hydrogen, and

5. The soundness or perfection of the structure of the α-Zr-H/solid solutions.

I

EXPERIMENTAL PROCEDURE

A

Materials used, Samples and Analyses

1. The Zr-hydride powder (grade R)(from metal Hydrides, Incorporated, Beverly, Mass.) had the following chemical composition in % by weight:

Zr - 97.8	Al - 0.002
Hf - 0.005	Ca - 0.001
H - 1.95	Mg - 0.01
O - 0.12	Fe - 0.06
N - 0.01	Cr - 0.0075
C - <0.01	Ni - 0.002
Cl - <0.003	Mn - 0.002
B - <0.00005	Ti - 0.0015
Si - 0.003	

For the tensile strength determinations a 0.5 mm thick Zr-wire with a minimum guarantee of 99.5% Zr (obtained from the H. Cross Company, Weehawken, N. J.) was used. The H-content of the Zr-hydricle was checked by the hydrogen evolution method[13] with the result: the average H-content (of 3 determinations)

was 2.08% H_2; or the average composition of the Zr-hydride was $ZrH_{1.88 \pm 0.06}$, while from the analysis as given above a composition of $ZrH_{1.77}$ resulted. The agreement is fairly good.

2. Preparation of the Zr - H samples. The Zr-H samples containing various amounts of H were prepared in an apparatus shown in Fig. 2. It consists of three main sections: of a source delivering pure H_2; of a tube for loading the Zr with H, and of a vacuum pumping system. $ZrH_{1.88}$ powder in the Al_2O_3-boats was placed into quartz glass tubes I and II. Then the whole system was evacuated down to 5 μ Hg; the adsorbed gases were released by heating the glass walls from the outside with a Bunsen burner and finally tube I was heated up to 600°C to fill the whole system with pure hydrogen. The latter was pumped off and the same procedure was repeated several times, so that the remaining oxygen content became negligible. After that tube II was heated to temperatures between 750° and 1000° C for 1 to 3 hours to decompose the Zr-hydride and, depending on temperature and time, to obtain specimens with various hydrogen contents. Then the samples were slowly cooled to room temperature in the furnace in approximately 10 hours under vacuum, so that it could be assumed that the hydrogen dissolved in the Zr was equally distributed throughout the sample. The specimens were then analyzed. In this way samples with hydrogen contents in

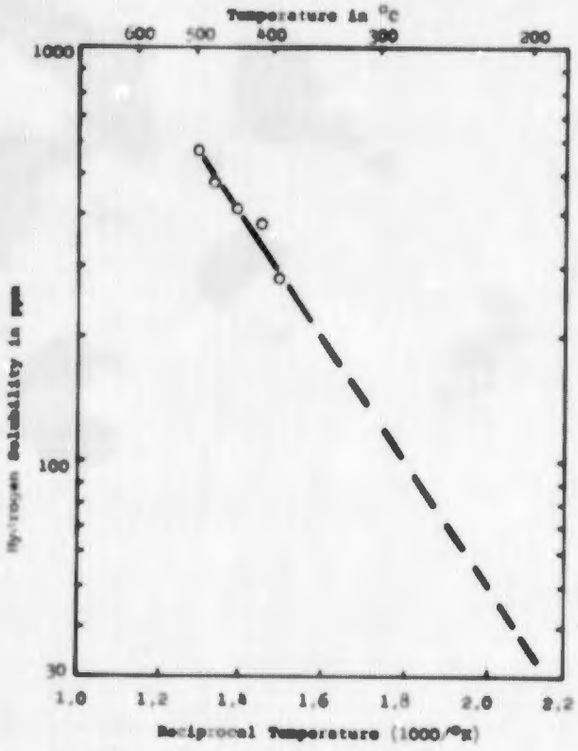

Fig. 1. Solubility of hydrogen in α-Sr at various temperatures and low hydrogen pressure (C.H.Schwartz and M.W.Mallett[1])

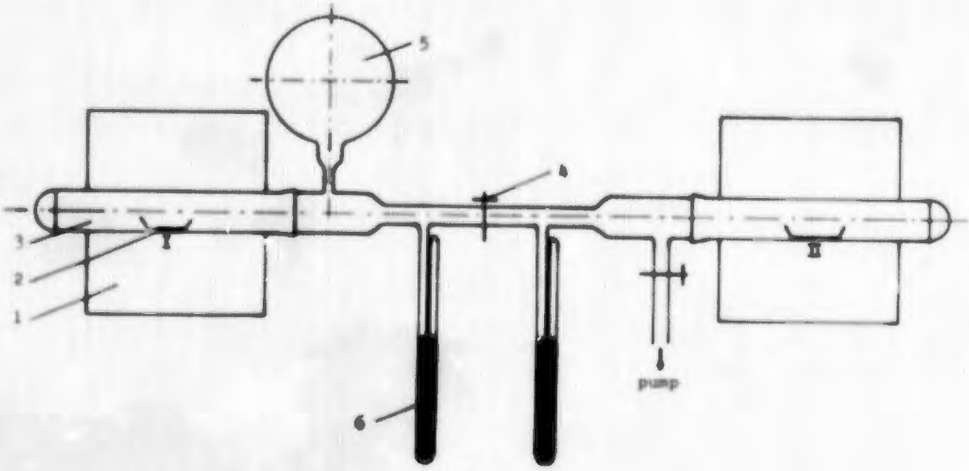

Fig. 2. Apparatus for the preparation of the Sr-H samples

1- Furnace, 2- Al_2O_3 boat, 3- Quartz tube, 4- Stopcock, 5- Expansion vessel, 6- Manometer

the range from 88 to 805 ppm were obtained. To drive out all the H_2, higher temperatures are necessary. However, at these temperatures the powder sintered together and precision parameter determinations were impossible.

The Zr wires were charged with various amounts of hydrogen (up to 500 ppm) in tube II by admitting to it various amounts of hydrogen evolved in tube I, after having annealed in tube II the originally cold drawn wires for 2.5 hours at 600°C under high vacuum. After the hydrogen absorption by the wires, the temperature of tube II was held at 600°C for 1 hour for H diffusion and equilabration.

3. Determination of the hydrogen content of the samples. For the determination of the hydrogen content the Leco hydrogen analyser was used. There the gas is removed by hot extraction in vacuum. A powder sample of ZrH_x or the wire was weighed in a stainless steel crucible and placed into the analyser which then was evacuated to a gas pressure of p_1 (normally zero), measured by a McLeod gauge. Then the sample was induction heated to 950°C for 10 min. and the increased pressure p_2, representing the total amount of the gases liberated from the sample, was read from the same gauge. All the gas was passed through a separation system for another 10 min. where the hydrogen was removed by oxidation to H_2O. The new pressure p_3 (of the residual gases) subtracted from p_2 gave the pressure

attributable only to hydrogen. Mostly 3 to 4 determinations of each sample were made and the average H content was calculated with an error of 3.9%.

B

The Asymmetric Diffraction Powder Patterns.

By loading the powder camera with a film in the asymmetric position, the circumference of the film can be exactly determined without knowing the diameter of the camera or the degree of film shrinkage after its development. Careful sample mounting, centering and maintenance of a constant and known temperature of the sample during exposure make it possible to measure the lattice parameter of crystalline powders with high precision. A detailed description of the experimental method and the necessary equipment is given in the literature[14-16].

1. Sample mounting. All the powder samples for X-ray diffraction were sieved through a 325 mesh screen. These powders were attached to the surface of a lithium-boron glass fiber (0.05 mm in diameter and 5-8 mm in length) coated with a uniform and thin layer of oil. The powder was uniformly spread over a few millimeters of the glass fiber and the mount carefully centered and aligned. Such well-centered, thin, uniform, and undistorted crystalline powder mounts yield sharp diffraction lines. If it was necessary to remove the powder from the glass fiber,

a small amount of acetone was applied to the oil of the fiber by means of a thin aluminum foil. The acetone dissolved the oil which held the powder, and the powder, rotating the glass fiber, could easily be removed from the fiber. The clean glass fiber was then ready for another powder mount.

All these operations were carefully performed under a microscope.

2. Indexing of the patterns and the selection of the proper radiation. The pattern of Zr was indexed analytically[17]. Co-radiation (without filtration) was found to be the proper one.

Zr has an hexagonal structure at room temperature and has the following lattice constants:

$a = 3.231$ Å and $c = 5.148$ Å.

The $\sin^2\theta$ values calculated with these constants and the respective line indexes for the Zr-pattern are listed in Table I.

3. X-ray diffraction patterns. The film was loaded asymmetrically in the powder camera (64 mm in diameter) and two holes were carefully drilled into the film to admit the collimator and the beam stopper. Drilling was preferred to punching, because punching of holes causes an uneven local shrinkage of the film[19].

The loaded camera was mounted in a thermostat which was capable of maintaining constant temperatures within ± 0.05°C. When the desired temperature was reached an additional hour was taken to assure temperature constancy of the sample before

TABLE I

Indexing of the Zr-powder pattern. Co-rad.

Line	$\sin^2\theta$ obs.	Calc.	hkl
1	0.1026	0.1022	100
2	0.1207	0.1208	002
3	0.1326	0.1324	101
4	0.2234	0.2230	102
5	0.3067	0.3066	110
6	0.3743	0.3740	103
7	0.4199	0.4188	200
8	0.4394	0.4390	201
9	0.4844	0.4832	004
10	0.5301	0.5296	202
11	0.5852	0.5854	104
12	0.5795	0.6806	203
13	0.7145	0.7154	210
14	0.7442	0.7456	211
15	0.7882	0.7898	114
16	0.8341	0.8362	212
17	0.8549	0.8572	105
18	0.8892	0.8920	204
19	0.9166	0.9198	300
20	0.9840	0.9872	213

exposure. Two photographs were taken at each constant temperature ranging from 15 to 55° in increments of about 10°. The exposure time was 1.5 hrs. The same film processing was maintained throughout this work.

4. Film measurement. The diffraction lines were measured using a comparator with a resolving precision of 0.002 mm and for some films with broader lines a microdensitometer of a precision of 0.02 mm. The film was placed between the two glass plates of the comparator of microdensitometer and was so adjusted that the

cross hair of the microscope or the beam of the microdensitometer traveled along the equator of the diffraction line pattern.

Two sets of lines in the front and back reflection regions were measured and from these measurements the effective film circumference, the conversion factor (from mm to degrees) and the back reflection Bragg-angles were calculated[14, 20].

5. Lattice constants. The lattice constants for the hexagonal ZrH_x were calculated from the usual equations. However, as for the calculation of the a constant the α_1 line of the index 300 (Table I), falling under a Bragg angle $\theta_2 = 73°$ could be used, the respective equation was simply:

$$a = \lambda^2/3(\sin^2\theta_2/9)^{1/2} \qquad (1)$$

The c constant could then be calculated, using the last interference 213 (Table I) and the respective angle θ_1 (= about 83°), from the equation (2) and (3):

$$c = \lambda^2/4[(\sin^2\theta_1 - 7A)/9]^{1/2} \qquad (2)$$

where

$$A = \sin^2\theta_2/9 \qquad (3)$$

The wave length λ used was that of $Co\alpha_1$ = 1.78529 kX. The lattice parameters were later converted into Å by multiplying them with 1.00202.

6. Coefficients of thermal expansion. The coefficients α_a and α_c (in the direction of the a- and c-axis respectively)

were determined from the average lattice constants at different temperatures, using the following equation:

$$\alpha_a = \Delta a/a \cdot t \qquad (4)$$

and

$$\alpha_c = \Delta c/c \Delta t \qquad (5)$$

$\Delta a/\Delta t$ and $\Delta c/\Delta t$ are the thermal expansivities of the unit cell and are represented by the slopes of the straight lines in the plots of the lattice constants versus temperature. The coefficients of thermal expansion were calculated from them and the lattice constants reduced to those at 25°C.

7. Diffraction correction. The wave lengths of X-rays are altered by refraction when they pass from one medium to another. In order to correct for refraction, the calculated cell dimensions are divided by the refractive index n of the material. The refractive index n can be found from the equation:

$$n = 1 - (2.71 \times 10^{-6} \cdot d \cdot \Sigma A / \Sigma W) \qquad (6)$$

Where d is the density of the material, ΣA - the sum of atomic numbers and ΣW - the sum of the atomic masses of the constituent elements of the unit cell. Frequently it turns out that the refr. corr. is within the limits of error of the determinations.

8. Error Calculation. In order to evaluate the precision of the lattice constant determination, error calculations are necessary. The values of lattice constants measured at different temperatures were reduced to constants at 25°C, using the

coefficients of thermal expansion α_a and α_c. The deviations from the average values were calculated, and the standard deviations and most probable errors were found from equations (7) and (8):

$$s' = \left[\sum (x)^2/(n^1-1)\right]^{1/2} \quad (7)$$

$$s = 0.6758^{t} \quad (8)$$

C

Density Determinations. For the determination of the structural perfection of the Zr-H solid solutions, accurate density measurements were necessary. The method was essentially, with certain modifications, that of Baker and Martin[22] based on Archimedes' principle.

The Zr-H powder samples were placed in a small silver crucible attached to a thin platinum wire with a hook at its end for suspension. The following operations were performed:

1) The sample was suspended in a beaker of xylene and placed in a vacuum desiccator equipped with a vibrator;

2) The powder was outgassed using mechanical vibration and vacuum;

3) The beaker was removed from the desiccator, the sample and its container were weighed while still immersed in the xylene, and the temperature of the xylene was recorded at the time of weighing;

4) The xylene was then completely evaporated from the sample and a second weighing was made in air with an accuracy of 0.0002 g. Knowing the density of xylene (as a function of temperature), the densities were calculated from the equation:

$$d = (d_x - d_a)(b-c)/\left[(b-c)-(d-e)\right] + d_a \qquad (9)$$

where d is the density of the sample, d_a the density of air, d_x the density of xylene, (b-c) the weight of the sample in air and (d-e) the weight of the sample in the liquid. The addition of the last term d_a gave the density of the sample in vacuo.

D

Tensile properties. For the investigation of the influence of the hydrogen on the tensile properties of a Zr-wire, tensile tests with 0.5 mm thick and 200 mm long wire specimens were carried out at room temperature on a "Instron Universal Tensile Testing Machine." The speed of testing was 0.2 in/min. The applied load was shown on a recorder with an accuracy of 0.1 lb., and the elongation was measured by cross-head travel. In order to determine the tensile strength, the maximum load was read from the recorded load-strain diagram and divided by the diameter of the wire of 0.5 mm. The yield strength was calculated by dividing the 0.2% offset-load by the diameter. The elongation was obtained in % per original gage length (1.5 in).

II

EXPERIMENTAL RESULTS

A

Lattice Parameters and Coefficients of Thermal Expansion.

For the determination of the thermal expansivity, a Zr-sample was used containing 122 ppm H. The averages of two lattice constants are plotted versus temperature in Fig. 3. From the slopes of these plots, calculated by the method of the least squares, the coefficients of thermal expansion were derived:

$$\alpha_a = 4.5\times10^{-6} \text{ and } \alpha_c = 11.0\times10^{-6} (^\circ C^{-1})$$

These values, obtained between 15 and 65°C, are consistant with those of the literature: McGreany and Lustman[23] mention the coefficients

$$\alpha_a = 5.5\times10^{-6} \text{ and } \alpha_c = 10.3\times10^{-6}$$

while Skinner and Johnson[24] found

$$\alpha_a = 5.5\times10^{-6} \text{ and } \alpha_c = 10.8\times10^{-6} {}^\circ C^{-1}.$$

The average lattice constants found for Zr (containing 122 ppm H) from the measurement of 10 films are as follows:

$$a_{25} = 3.23622 \pm 0.00005 \text{ and } c_{25} = 5.1526 \pm 0.0003 \text{ Å}$$

corrected for refraction. The refractive index n was 0.999975 and the correction was within the limits of errors for the c constant.

B

Lattice Constants as a Function of the Hydrogen Content of α-Zr. As stated in the previous chapter, Co $K\alpha_1$-radiation and the (300) and (213) lines were used for the determination of the precise lattice constants. Since the (300)-line was frequently rather weak and the (213)-line was broad, the measurements were made with the microdensitometer. Nevertheless, the error was larger than found for sharp lines measured with the comparator.

The lattice constants obtained with α-Zr at 25°C of various hydrogen contents are listed in Table II. The average of two lattice constant determinations is plotted against the hydrogen content in Fig. 4.

The parametric method is based on the fact that the lattice parameter of a solid solution generally changes along a straight line with the composition up to the saturation limit, and then remains constant. The limit of the solid solution region is given by the intersection of the two branches of the parameter curves. This limit is estimated to be - as can be seen from Fig. 4 - at 310 ppm H at room temperature, independent of the H pressure. The effect of increasing hydrogen content on the dilatation along the c-axis is more pronounced than that along the a-axis, as the a-parameter remains nearly constant. However,

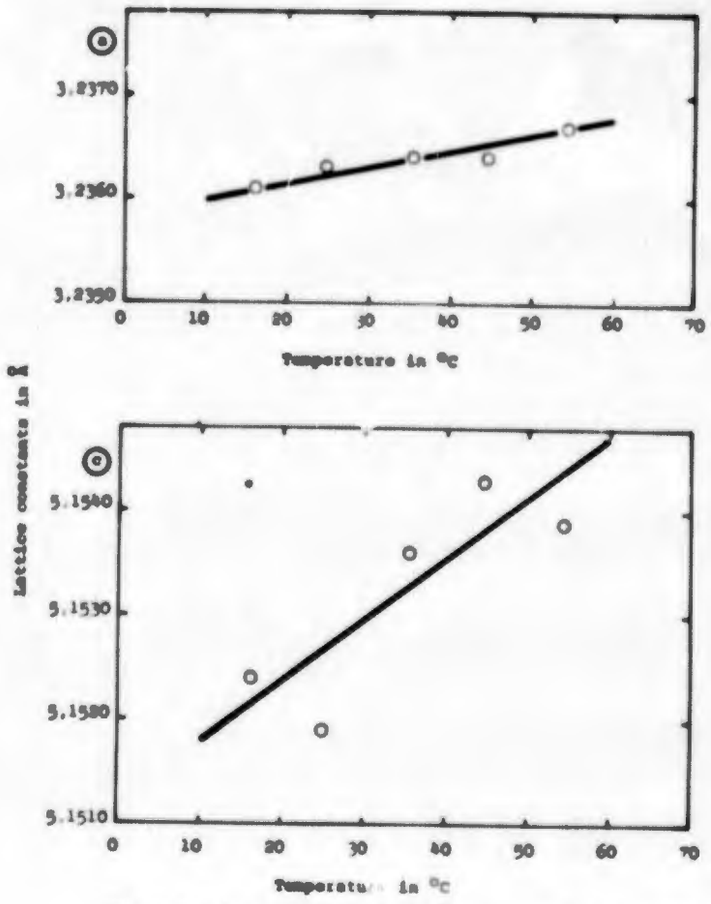

Fig. 3. Lattice constants versus temperature (Hr = 122 ppm H)

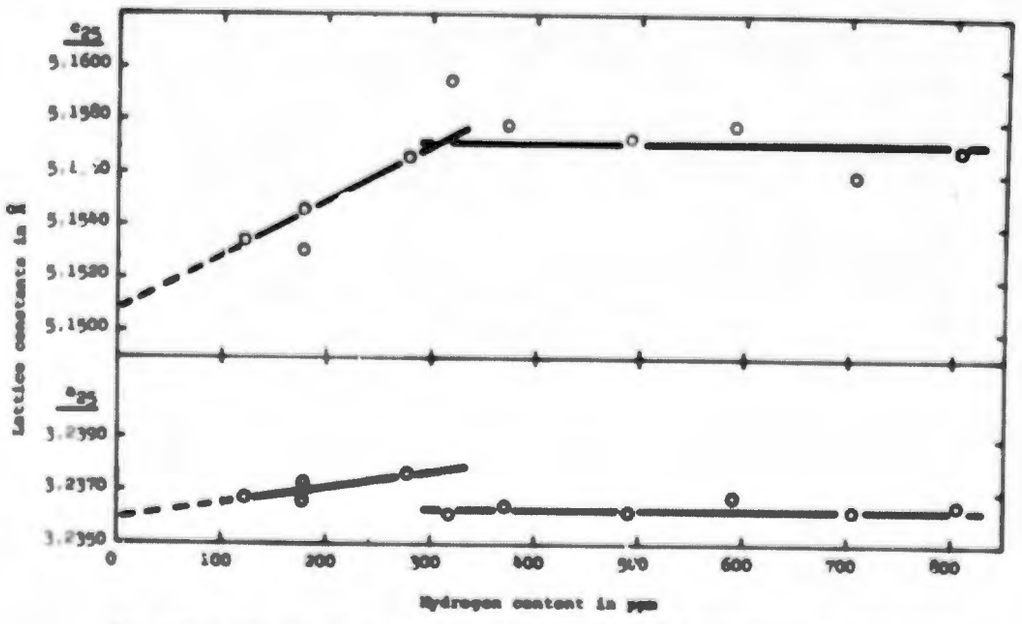

Fig. 4. Lattice constants versus hydrogen content at room temperature, independent of the hydrogen pressure

Table II

Average lattice constants a and c, (divided by the refractive index n = 0.999975) of Zr containing various hydrogen amounts at 25°C. Co-radiation.

Film No.	Hydrogen contents in ppm	Average a_{25} in Å	Average c_{25} in Å
2550 2551	122	3.2368	5.1535
2562 2563	177	3.2367	5.1547
2566 2567	178	3.2374	5.1531
2564 2565	277	3.2377	5.1567
2568 2569	318	3.2362	5.1596
2560 2561	371	3.2365	5.1579
2556 2557	490	3.2363	5.1574
2554 2555	590	3.2369	5.1579
2552 2553	705	3.2364	5.1560
2559	805	3.2366	5.1570

there is a clear discontinuity at about 300 ppm.

The lattice parameters of pure Zr can now be found by extrapolation:

$$a_{25} = 3.2360 \text{ and } c_{25} = 5.1508 \text{ Å}.$$

c

The Density as Function of the Hydrogen Content in α-Zr.

The density versus hydrogen content is plotted in Fig. 6. The first point (at a H content = 0) is the x-ray density d_x of

pure Zr calculated from the equation:

$$d_x = Mn/vN_o \qquad (10)$$

where M is the molecular weight of Zr, v - the volume of the unit cell of Zr calculated from the extrapolated a and c values of Fig. 4; N_o - Avogadro's number (6.024×10^{23} mole^{-1}), and n the ideal number of atoms per unit cell, namely six. d_x was found to be 6.484 g/cm^3 at 25°C, which agrees closely with the literature data[25] (d_{20} = 6.4 g/cm^3 ±0.001, reduced to 25°C: d_{25} = 6.489 g/cm^3).

The densities of the following hydrogen containing Zr-samples were determined using the method described in the previous chapter: Zr containing 88, 102, 118, 133, 178, 241, 277 and 300 ppm H. All these compositions are within the solid Zr-H solution range, as can be seen from Fig. 4. First the densities were measured at the experimental temperatures, then these values were reduced to the density at 25°C, d_{25}, using equation (11)

$$d_{25} = d_t/[1 - \beta(25 - 5)] \qquad (11)$$

where d_t is the density of the sample at the temperature t°C during the measurement, and β - the thermal volume expansion coefficient, which is $(2\alpha_a + \alpha_c)$. For ZrH_x β was calculated to be 20.2×10^{-6} °C^{-1}. However, the reduction of density from the working temperature to 25°C only affects the fourth decimal.

The average densities at 25°C of the eight samples, obtained in ten determinations of each one, are listed in Table III.

Table III

Densities of eight ZrH_x samples at 25°C.

H-content in ppm	x in ZrH_x	d_{25} in g/cm^3
0*)	0.0	6.484*)
88	0.008	6.459±0.002
102	0.009	6.475±0.002
118	0.0107	6.479±0.002
133	0.012	6.481±0.004
178	0.016	6.455±0.004
241	0.022	6.451±0.002
277	0.025	6.469±0.004
300	0.027	6.456±0.003

*) X-ray density.

A temperature of 1000°C was necessary to reduce the H content to 88 ppm. The weights of the samples used were in the range of 0.64 to 0.98 g.

Fig. 6 shows that the density of pure Zr is the highest. With increasing H content the densities seem to decrease. The considerable fluctuations are due to the difficulties in the density determinations of small hydrogen containing powder samples. Although about 100 density determinations were made, better results could not be achieved. There was no reaction between xylene and Zr.

D

Tensile Properties as Function of the H Content in Zr. The tensile properties of Zr wires with various hydrogen contents were determined using the method described in the previous chapter. The composition of the wires and their tensile properties are summarized in Table IV. The samples containing up to 270 ppm were in the solid solutions range (see Fig. 4); those containing 409 and 496 ppm H were already in the two-phase region. Table IV shows that the Zr wire as received, being strongly cold deformed, has a high yield and tensile strength and low elongation values, while the annealed Zr wires exhibit a low yield and tensile strength slightly increasing with increasing H contents in the solid solution range. In the two-phase region there is a stronger increase of the yield and tensile strength with increasing H concentration, as shown in Fig. 5. The elongation values which are relatively high in the annealed compared with the unannealed condition, decrease uniformly with increasing H contents.

The results are partly consistent with the literature[26] where up to 500 ppm H a slight increase of the yield strength and a decrease of the elongation with increasing H contents has been reported. The tensile strength of unalloyed Zr, however, was found to increase slightly up to 200 ppm H and to

decrease then slightly up to 500 ppm H. The authors of reference 26 consider the yield and tensile strength up to 500 ppm H to remain about constant.

TABLE IV

Tensile properties of Zr wire as received and of annealed Zr wires containing various amounts of hydrogen at room temperature

x in ZrH_x	H-content in ppm	Tensile Strength in psi	Average	Yield Strength in psi	Average	Elongation in %	Average
0.002	20*	111000		102000		9	
		110000	110300	99300	98900	10	9
		110000		95400		7	
0.002	20**	56400		26800		25	23
		55400	55900	29300	28100	20	
0.013	140	55700		27900		28	
		56100	56100	28200	28100	23	26
		56400		28200		27	
0.021	229	57100		30000		24	
		57900	57300	27900	28700	22	23
		56800		28500		24	
0.024	270	56400		29600		20	
		56400	56400	28600	29100	21	21
0.037	409	58900	58900	30000	31500	19	
		58900		32900		21	20
0.045	496	60700		30700		23	
		60000	60400	30700	30700	20	22

* as received
** annealed in vacuo

III

DISCUSSION

1. Extent of Solid Solubility of Hydrogen in α-Zr at Room Temperature. The solubility of H in α-Zr at room temperature has not yet been determined directly. All the data available about this subject resulted, as already mentioned, from extrapolations of H solubility at higher temperatures (>300°C) to room temperature (Fig. 1) and was estimated to be in the range of 10 ppm. at low H pressures (0.1 - 4 Hg)[1,10]. In this investigation, using the parametric x-ray method, a much higher H solubility limit in α-Zr was found, namely 310 ppm. but independent of the H pressure.

This H solubility limit could not be influenced by the solubility of oxygen in α-Zr, because firstly, there was no oxygen present in the apparatus, secondly the terminal solubility of oxygen in α-Zr at room temperature is much higher (approximately 6.8% b.w.[27]), and thirdly the change in lattice parameters with oxygen present would be larger. Besides, the oxygen would decrease the solubility of H in α-Zr[5,28,29,30,31]. Therefore it can be concluded that the change in lattice parameter up to 310 ppm H is caused by the hydrogen being in solid solution. The more pronounced effect of dissolved H on the c- rather than on the a-parameter can be explained by the location of the

H-atoms within the tetrahedral interstices in the hexagonal close-packed structure of α-Zr[30]. Therefore, the dissolved H-atoms must expand the lattice more in the direction of the c-axis than in the direction of the a-axis. However, in order to explain the expansion and then the contraction of the a constant with increasing H-concentration in Zr (Fig. 4), it can be assumed that the H-atoms may also go into the octahedral holes in small amounts. Then, as soon as the hydride phase is formed (at larger H concentrations) the H leaves the octahedral holes and joins the new phase because this may be energetically more advantageous for the octahedral hydrogen. Simultaneously the a constant of the saturated α-Zr drops nearly to the value of pure Zr. Of course, this is one possibility of explanation for the effect if it will turn out to be real. A similar situation is found in the systems Al-Au[32] High diffusion rates of H in Zr and slow cooling further the breakdown of supersaturated states[1]. But even air cooling below 315° causes hydride precipitation.

Further proof for the high solubility limit of H in Zr was the tensile strength. Fig. 6 shows a bend in the tensile strength vs. H-content curve at about $x = 0.025$ of ZrH_x which corresponds to an H-content of about 280 ppm. Assuming that the sharp bend represents the solubility limit of H in α-Zr, about the same

results are obtained as with the lattice parameter method (see upper curves Fig. 5). The small effect of low H-concentrations (within the solid solubility in Zr) upon the tensile strength, agrees with the reports in the literature[25,33,34].

ii. Perfection of the Crystal Structure as a Function of the H Content in -Zr. If the H-atoms in the solid solution are going into the interstices of the Zr lattice and if the latter is thereby expanded moderately, a density increase should be expected for the solid solution with H increase. However, Table III and Fig. 6 show a decrease in density with increasing concentration of H. Although the experimental points in Fig. 6 fluctuate, nevertheless a definite decrease in density is apparent, as verified by the straight line calculated with the method of least squares. If the expansion of the lattice would compensate the density increase due to the built in hydrogen, the experimental density should be equal to the x-ray density, or both densities should run parallel with increasing hydrogen content of the solution. The x-ray densities d_x of the various solid solutions were calculated from eq. (10). They are summarized in Table V and plotted in Fig. 6.

As can be seen from the plot of Fig. 6, all the d_x values are on one straight line, meaning that the analyses and the lattice constant determinations are correct within the limits

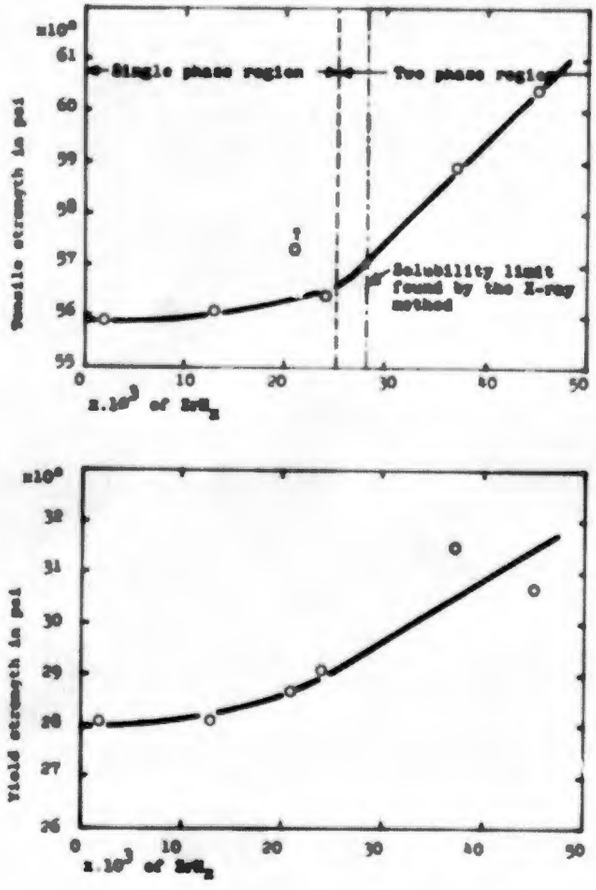

Fig. 5. Tensile properties versus hydrogen content of ZrH_x

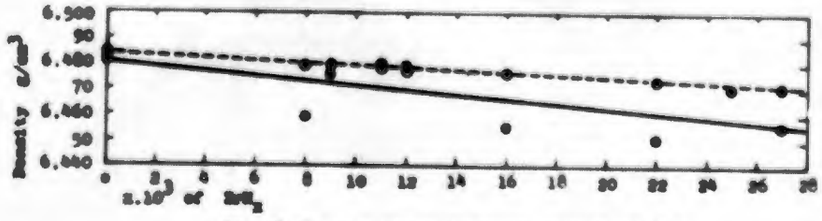

Fig. 6. Density versus hydrogen content of ZrH_x

● - x-ray density
● - experimental density

TABLE V

X-ray densities d_x of 9 ZrH_x samples calculated from eq.(10). n = 6, $N_o = 6.024 \times 10^{23}$, Δ = difference

in ZrH_x	M of ZrH_x	V in $Å^3$	d_x $g\ cm^{-3}$	d_{obs} $g\ cm^{-3}$	Δ
0.0	91.22	140.130	6.4837	6.481*	0.0027
0.008	91.228	140.231	6.4796	6.459	0.0206
0.009	91.229	140.236	6.4795	6.475	0.0045
0.011	91.231	140.256	6.4787	6.479	-0.0003
0.012	91.232	140.275	6.4779	6.481	-0.0031
0.016	91.236	140.323	6.4760	6.455	0.021
0.022	91.242	140.376	6.4739	6.451	0.0229
0.025	91.245	140.438	6.4713	6.469	0.0023
0.027	91.247	140.443	6.4712	6.456	0.0152

*Extrapolated value

of error. Although the scatter of d_{obs} is rather large, nevertheless, as shown by Table V, all the observed values, except two are <u>below</u> the calculated ones, indicating that vacant sites or even agglomerations of such sites are formed in the Zr structure during the absorption of H. As in all these measurements the powder at the temperatures used never sinctured together, formation of larger holes inside the grains was excluded. Therefore, it has to be assumed that the decrease in density is due to another vacant site concentration being in equilibrium with Zr and H.

The number of such sites can be calculated from eq. (10) writing it as follows:(35)

$$n' = vdN_o/M \qquad (11)$$

where n' is now the actual number of ZrH_x molecules unit cell

and d is the experimental density. The solid line of Fig. 6, representing the experimental densities, and which was drawn according to least squares calculation, passes closely the third and the last point of the diagram (the densities 6.475 and 6.456 g cm^{-3}). From these two values the actual number n' of molecules per unit cell is calculated to be 5.9958 and 5.9859, which is also the number of Zr atoms per u. c. Therefore the number of vacant sites in the main Zr lattice increases from nearly zero through 0.004 to 0.014 sites/u.c. with increasing H-concentration in the metal up to the point of saturation, while the hydrogen is going into the interstices.

iii. Mechanical Properties of the Zr-H Solutions. When Zr at a certain temperature becomes saturated with H and when there is still a sufficient H-gas pressure, the formation of a second phase, that of the hydride, starts. The vacancies within the Zr lattice or the agglomerations of vacancies can well serve as nucleation centers for the new phase. This phase, however, has a lower density[36] than the saturated Zr phase (4.9 for $ZrH_{1.5-2}$ versus 6.456 g cm^{-3}, see Table V) and will occupy a larger space than is available. Therefore, after the vacancy agglomerations have been filled with the new hydride phase, microcracks will originate upon further growth of the hydride

nuclei. But the presence of microcracks changes the mechanical properties and causes the brittleness of the Zr supersaturated with H.

It was further found that the tensile and yield strength increased slightly in the solid solution range and strongly in the two-phase region with increasing H-content, while the elongation decreased uniformly with increasing H-content, as shown in Table VI and Fig. 5. The slight increase of the strength may be due to the fact that the lattice is strained by the dissolved H-atoms. This does not contradict the fact that the number of vacant sites increases with increasing H-content in s lid solution. The effect of straining the lattice overbalances the strength reducing effect of an increasing number of vacant sites in the lattice.

The strong increase in the two-phase region can be explained by the interpretation Westlake gave for the results of his investigation[37]. He showed that hydride aciculae in Zr are satisfactory obstacles to the dislocation motion. He presented further evidence that the stress at the head of a dislocation pile-up must be higher than in the case of unalloyed Zr and that this is sufficient to fracture the hydride and thus nucleate a crack in the surrounding Zr matrix, which in turn is responsible for the low ductility. However, as shown in the present

investigation, the formation of cracks is furthered by the growth of hydride aciculae requiring a larger space than available in the Zr matrix saturated with hydrogen.

ACKNOWLEDGEMENTS

The authors are thankful to Mr. J. A. Rowland, Research Director at the Rolla Metallurgy Research Center, for his permission to conduct the tensile tests of this investigation, using the facilities of the Center.

REFERENCES

1. C. M. Schwartz and M. W. Mallett, Trans. Am. Soc. Metals, 46, 640 (1954).
2. W. L. Mudge, Jr., "Zirconium and Zirconium Alloys" American Soc. Metals, Cleveland, p. 146 (1953).
3. A.D. Schwope, ibid., p. 292.
4. J.H. de Boer and J.D. Fast, Rec. trav. chim., 55, 459 (1936).
5. M.N.A. Hall, S.L.H. Martin, and A.L.G. Rees, Trans. Faraday Soc., 41, 306 (1945).
6. E. A. Gulbransen and K. F. Andrew, J. Metals, 7, 136 (1955).
7. R.K. Edwards, P. Levesque, and D. Cubicciotti, J. Am. Chem. Soc., 77, 1307 (1955).
8. D. A. Vaughan and J. R. Bridge, Trans. AIME, 206, 529 (1956).
9. C. E. Ells and A. D. McQuillan, J. Inst. Metals, 85, 89 (1956/57).
10. M. W. Mallett and W. M. Albrecht, J. Electrochem. Soc., 104, 142 (1957).
11. G. G. Libowitz, J. Nucl. Materials, 5, 228 (1962).
12. J. Motz, Z. Metallk. 53, 770 (1962).
13. M. E. Straumanis and T. Ejima, Z. analyt. Chem., 177, 241 (1960).
14. M. E. Straumanis and A. Ievinš, "The Precision Determination of Lattice Constants by the Asymmetric Method", Goodyear Atomic Corp., Portsmouth, Ohio (1959).
15. M. E. Straumanis and E. Z. Aka, J. Appl. Phys., 23, 330 (1952)
16. M. E. Straumanis and E. Z. Aka, J. Am. Chem. Soc., 73, 5643 (1951).
17. B. D. Cullity, "Elements of X-Ray Diffraction", Addison-Wesley Publishing Company, Inc., p. 311 (1959).

18. R. B. Russell, Trans. AIME, 200, 1045 (1954).
19. M. H. Jellinek, Rev. Sci. Instrument, 20, 368 (1949).
20. M. E. Straumanis in G. L. Clark's "Encyclopedia of X-Rays and Gamma Rays," Reinbold Publ. Corp., New York 1963, p. 700.
21. N. F. Henry, H. Lipson, and W. A. Wooster, "The Interpretation of X-Ray Diffraction Photographs, The MacMillan Company, London, p. 29 (1951).
22. I. Baker and G. Martin, End. Eng. Chem. Anal. Ed., 15, 279 (1943).
23. R. K. McGeary and B. Lustman, Trans. AIME, 191, 994 (1951).
24. G. B. Skinner and H. L. Johnston, J. Chem. Phys., 21, 1383 (1953).
25. H. K. Adenstedt, Trans. Am. Soc. Metals, 44, 949 (1952).
26. D. Weinstein and F. C. Holtz, Trans. Quarterly Am. Soc. Metals, 57, 284 (1964).
27. M. Hansen, D. J. McPherson, and R. F. Domagala, Report C00-123 (1953).
28. M. E. Straumanis, W. J. James and C. S. Lin, J. Appl. Chem. 10, 389 (1960).
29. C. F. Bevington, S. L. Martin and D. H. Mathews, Proc. Intern. Congr. Pure and Appl. Chem., 11, Congr. London, 1947, 1, 3 (1950).
30. R. E. Rundle, C. G. Shull and E. O. Woolan, Acta. Cyst. 5, 22 (1952).
31. S.L.H. Martin and A.L.G. Rees, Trans. Farad. Soc. 50, 343 (1954).
32. M. E. Straumanis and K. S. Chopra, Z. Physik. Chem. 1964.
33. J. Fitzpatrick and H. P. Roth, Repot MIT-1078 (April 1952).
34. W. J. Babyak, W. F. Bourgeouis and G. J. Salvaggio, WAPD-275 (Nov. 1963).
35. M. E. Straumanis in G. L. Clark's "Encyclopedia of X-Rays and Gamma Rays", Reinbold Publ. Corp., New York 1963, p. 733.
36. B. Lustman and F. Kerze "The Metallurgy of Zirconium", McGraw-Hill Book Co., New York, 1955, p. 287.
37. D. G. Westlake, Tr. Quart. Am. Soc. Met. 56, 1 (1963).